C_2H_4 Insertion into Pt^{II}–SiH_3 and Pt^{II}–H Bonds. An ab Initio MO/MP4 Study

Shigeyoshi Sakaki,* Masahiro Ogawa, Yasuo Musashi, and Toru Arai

Contribution from the Department of Applied Chemistry, Faculty of Engineering, Kumamoto University, Kurokami, Kumamoto 860, Japan

Received February 7, 1994®

Abstract: Insertion reactions of C_2H_4 into the Pt–H and Pt–SiH_3 bonds of a platinum(II) hydride silyl ethene complex, $PtH(SiH_3)(PH_3)(C_2H_4)$, are investigated with the ab initio MO/MP4SDQ method. When the H ligand lies at the position trans to C_2H_4, C_2H_4 is inserted into the Pt–SiH_3 bond with a significantly high activation energy (E_a) of 54 kcal/mol. When SiH_3 lies at the position trans to C_2H_4, C_2H_4 is inserted into the Pt–H bond with much lower E_a (21 kcal/mol). Although the product just after the insertion involves a strong Pt–H^β agostic interaction, deinsertion of C_2H_4 occurs with nearly no barrier. To complete hydrosilation of ethene, further conversion to the most stable product must occur by breaking the agostic interaction of about 17 kcal/mol. The total E_a of 38 (21 + 17) kcal/mol is lower than the E_a of the above-mentioned C_2H_4 insertion into the Pt–SiH_3 bond. When PH_3 is at the position trans to C_2H_4, C_2H_4 is inserted into the Pt–SiH_3 bond with E_a of 16.2 kcal/mol and into the Pt–H bond with E_a of only 4.4 kcal/mol. These results lead to the conclusions that ethene is much more easily inserted into the Pt–H bond than it is into the Pt–SiH_3 bond and that the Pt-catalyzed hydrosilation of alkene proceeds through the Chalk–Harrod mechanism. Determining factors for the ease of the insertion are the Si–C and C–H bond energies, the trans-influence of the ligand at the position trans to C_2H_4, the directionality of valence orbitals of H and SiH_3, and sometimes the agostic interaction between Pt and the C_2H_5 group formed in the reaction.

I. Introduction

The insertion reaction of alkene into M–H and M–SiH_3 bonds is of fundamental importance in the chemistry of hydrosilation of alkene.[1] For instance, it has been actively discussed whether alkene is inserted into the M–H bond (Chalk–Harrod mechanism)[1-3] or into the M–SiH_3 bond (modified Chalk–Harrod mechanism).[4] In this regard, detailed knowledge of the alkene insertion into the M–H and M–SiH_3 bonds is necessary for understanding well the hydrosilation of alkene and making further developments in the catalytic synthesis of Si compounds. Theoretical investigation is expected to offer valuable information, including the geometry of transition state, the activation energy, the energy of reaction, electron redistribution, etc., of the alkene insertion into M–SiH_3 and M–H bonds. However, the alkene insertion into the M–SiH_3 bond has not been theoretically investigated to our knowledge.

In this work, insertion reactions of C_2H_4 into the Pt–SiH_3 and Pt–H bonds of a platinum(II) hydride silyl ethene complex, $PtH(SiH_3)(PH_3)(C_2H_4)$ (**1**), are theoretically investigated with the ab initio MO/MP4SDQ method. **1** is selected here because the

$$\underset{\mathbf{1}}{PtH(SiH_3)(PH_3)(C_2H_4)} \rightarrow Pt(CH_2CH_2SiH_3)(H)(PH_3) \text{ or } \rightarrow Pt(CH_2CH_3)(SiH_3)(PH_3) \quad (1)$$

insertion reaction of ethene into a metal–hydride bond has been theoretically investigated in similar four-coordinate Pt(II) and Pd(II) complexes,[5,6] and the ethene insertion has been experimentally[7,8] and theoretically[5] reported to occur easily in four-coordinate Pt(II) complexes. Our aims are (1) to show which bond easily undergoes the C_2H_4 insertion, Pt–H or Pt–SiH_3; (2) to estimate the activation energy (E_a) and the energy of reaction (ΔE); and (3) to clarify determining factors for the ease of the insertion.

II. Computational Details

Geometries of reactants, transition state (TS), and products were optimized at the Hartree–Fock (HF) level with the energy gradient technique, where a C_s symmetry constraint was adopted. Some geometries were reoptimized at the MP2 level. TS was determined by calculating the Hessian matrix. In all the calculations, the geometry of PH_3 was taken to be the same as the experimental structure of the free PH_3 molecule.[9] MP4SDQ calculations were performed with all core orbitals excluded from an active space. Although MP4SDTQ calculations were also carried out for several complexes in order to examine the contribution of triple excitations, no significant difference between MP4SDQ and MP4SDTQ was observed (vide infra). Gaussian 86[10] and 92[11] programs were used for these calculations.

* Abstract published in *Advance ACS Abstracts*, July 1, 1994.

(1) For instance, see: (a) Harrod, J. F.; Chalk, A. J. In *Organic Synthesis with Metal Carbonyls*; Wender, I., Pino, P., Eds.; John Wiley & Sons, Ltd.: New York, 1977; Vol. 2, p 673. (b) Speier, J. L *Adv. Organomet. Chem.* **1979**, *17*, 407. (c) Ojima, I. In *The Chemistry of Organic Silicon Compounds*; Patai, S., Rappoport, Z., Eds.; John Wiley & Sons: New York, 1989; p 1479.

(2) Chalk, A. J.; Harrod, J. F. *J. Am. Chem. Soc.* **1965**, *87*, 16.

(3) Recent reports supprt the Chalk–Harrod mechanism, for instance: (a) Caseri, W.; Pregosin, P. S. *J. Organomet. Chem.* **1988**, *356*, 259. (b) Hostetler, M. J.; Bergman, R. G. *J. Am. Chem. Soc.* **1990**, *112*, 8621. (c) Hostetler, M. J.; Butts, M. D.; Bergman, R. G. *Organometallics* **1993**, *12*, 65.

(4) Tilley, T. D. In *The Chemistry of Organic Silicon Compounds*; Patai, S., Rappoport, Z., Eds.; John Wiley & Sons Ltd.: New York, 1989; p 1415.

(5) Thorn, D. L.; Hoffmann, R. *J. Am. Chem. Soc.* **1978**, *100*, 2079.

(6) Koga, N.; Obara, S.; Kitaura, K.; Morokuma, K. *J. Am. Chem. Soc.* **1985**, *107*, 7109.

(7) (a) Clark, H. C.; Kurosawa, H. *Inorg. Chem.* **1972**, *11*, 1275. (b) Clark, H. C.; Jablonski, C.; Halpern, J.; Mantovani, A.; Well, T. A. *Inorg. Chem.* **1974**, *13*, 1541. (c) Clark, H. C.; Jablonski, C. R. *Inorg. Chem.* **1974**, *13*, 2213. (d) Clark, H. C.; Wong, C. S. *J. Am. Chem. Soc.* **1974**, *96*, 7213. (e) Clark, H. C.; Jablonski, C. R.; Wong, C. S. *Inorg. Chem.* **1974**, *14*, 1332.

(8) Ben-David, Y.; Portnoy, M.; Gozin, M.; Milstein, D. *Organometallics* **1992**, *11*, 1995.

(9) Herzberg, G. *Molecular Spectra and Molecular Structure*; D. van Nostrand Co. Inc.: Princeton, NJ, 1976; Vol. 3, p 610.

(10) Frisch, A. M. J.; Binkley, J. S.; Schlegel, H. B.; Raghavachari, K.; Melius, C. F.; Martin, R. L.; Stewart, J. J. P.; Bobrowicz, J. W.; Rohlfing, C. M.; Kahn, L. R.; DeFrees, D. J.; Seeger, R.; Whiteside, R. A.; Fox, D. J.; Fluder, E. M.; Topiol, S.; Pople, J. A. *Gaussian 86*; Carnegie-Mellon Chemistry Publishing Unit: Pittsburgh, PA, 1986.

(11) Frisch, A. M. J.; Trucks, G. W.; Head-Gordon, M.; Gill, P. M. W.; Wong, M. W.; Foresman, J. B.; Johnson, B. G.; Schlegel, H. B.; Robb, M. A.; Replogle, E. S.; Gomperts, R.; Andres, J. L.; Raghavachari, K.; Binkley, J. S.; Gonzalez, C.; Martin, R. L.; Fox, D. J.; DeFrees, D. J.; Baker, J.; Stewart, J. J. P.; Pople, J. A. *Gaussian 92*; Gaussian, Inc., Pittsburgh, PA, 1992.

0002-7863/94/1516-7258$04.50/0

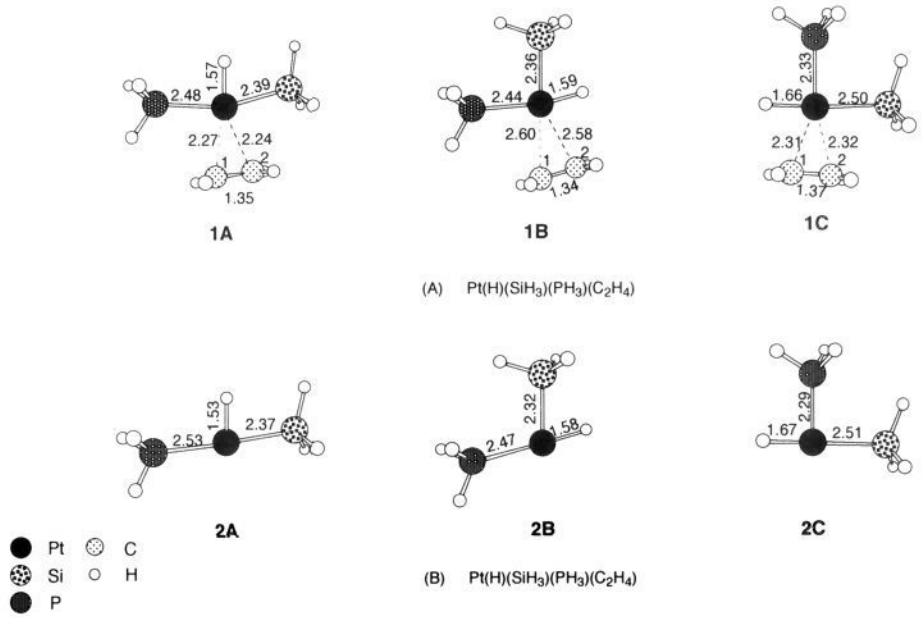

Figure 1. Optimized geometries of $PtH(SiH_3)(PH_3)(C_2H_4)$ (**1**) and $PtH(SiH_3)(PH_3)$ (**2**). Bond lengths in Å. Bond angles are omitted here for brevity.[17]

Two kinds of basis sets, BS I and BS II, were used in this work. In BS I, the core electrons (up to 4f) of Pt were replaced with the relativistic effective core potentials (ECPs) of Hay and Wadt, and the valence orbitals of Pt (5s, 5p, 5d, 6s, and 6p) were represented with a (5s 5p 3d)/[3s 3p 2d] set.[12] For C and Si, MIDI-3 sets were used,[13] while a MINI-1 set was employed for P.[13] A (4s)/[2s] set[14] was used for H, except H of PH_3, for which a minimal (3s)/[1s] set[15] was employed. In BS II, a (5s 5p 3d)/[3s 3p 3d] set was used for valence orbitals of Pt, where core electrons (up to 4f) of Pt were replaced with the same ECPs as in BS I.[12] For C, Si, and P, MIDI-4 sets were adopted.[13] A (4s)/[2s] set[14] was used for H. A p-polarization function ($\zeta = 1.0$)[14] was added to the basis set of an active H atom which coordinates to Pt only when it reacts with ethene. The basis set for Si was augmented with a d-polarization function in both BS I and BS II.[16]

III. Results and Discussion

Relative Stabilities of Three Isomers of $PtH(SiH_3)(PH_3)(C_2H_4)$ (1). There are three isomers in $PtH(SiH_3)(PH_3)(C_2H_4)$ (**1**), as shown in Figure 1:[17] C_2H_4 lies at the trans-position of H in **1A**, at the trans-position of SiH_3 in **1B**, and at the trans-position of PH_3 in **1C**. In **1A**–**1C**, ethene is on the molecular plane. The other structure, in which ethene is perpendicular to the molecular plane, is less stable than the in-plane structures by 2.0 kcal/mol for **1A** and **1B** and by 8.4 kcal/mol for **1C**. Although the energy difference between **1A** and **1B** is less than 0.1 kcal/mol (Table 1), **1C** is less stable than **1A** and **1B** by ca. 12 kcal/mol (at the MP4SDQ level).

Electron distribution and geometries of **1A**, **1B**, and **1C** will be inspected here to clarify the reason that **1C** is less stable than **1A** and **1B**. As compared in Table 1, electron populations of H and SiH_3 ligands of **1C** are larger but electron populations of PH_3 and C_2H_4 of **1C** are smaller than those of **1A** and **1B**. This means that **1C** involves the weaker charge-transfer interactions from H and SiH_3 to Pt and the stronger charge-transfer interactions from PH_3 and C_2H_4 to Pt than those of **1A** and **1B**. Consistent with this electron distribution, **1C** has the longest Pt–H and Pt–SiH_3 bonds and the shortest Pt–PH_3 bond among three isomers, as shown in Figure 1. These results clearly show that the H and SiH_3 ligands weaken the coordinate bond of the ligand lying at their trans-position; in other words, trans-influence of the H and SiH_3 ligands is strong. The strong trans-influence of the H and SiH_3 ligands is also reflected in the LUMO of $PtH(SiH_3)(PH_3)$ (**2**): its orbital energy (ϵ_{LUMO}) is 0.82 eV for **2A**, 1.12 eV for **2B**, and 0.26 eV for **2C**, where a vacant site is trans to H in **2A**, trans to SiH_3 in **2B**, and trans to PH_3 in **2C** (see Figure 1 for **2A**–**2C**). This LUMO consists mainly of the Pt dσ orbital, and an incoming ligand coordinates to Pt through the charge-transfer interaction with this LUMO. Because ϵ_{LUMO} increases in the order **2C** ≪ **2A** < **2B**, coordination of an incoming ligand would become strong in the order **2B** < **2A** ≪ **2C**. This means that the trans-influence becomes stronger in the order PH_3 ≪ H < SiH_3 (note that the coordination site is trans to H in **2A**, trans to SiH_3 in **2B**, and trans to PH_3 in **2C**). The situation of **1C** is the worst for the trans-influence because the H and SiH_3 ligands, both having strong trans-influence, lie trans to each other. This would be a main reason that **1C** is less stable than **1A** and **1B**. The trans-influence of H, SiH_3, and PH_3 ligands also exerts significant effects on the C_2H_4 insertion into the Pt–H and Pt–SiH_3 bonds, as will be shown below.

Table 1. Relative Energy (ΔE) and Electron Populations of $PtH(SiH_3)(PH_3)(C_2H_4)$ (**1**) and Energy Level of LUMO (ϵ_{LUMO}) of $PtH(SiH_3)(PH_3)$

	1A	1B	1C
ΔE^a (kcal/mol)	0.04	0.0[b]	12.2
electron population			
Pt	18.498	18.484	18.574
H	0.940	0.978	0.993
SiH_3	16.940	16.939	17.014
PH_3	17.769	17.733	17.596
C_2H_4	15.854	15.866	15.823
ϵ_{LUMO} (eV)	0.82	1.12	0.26

[a] MP4SDQ. A positive value means destabilization in energy (vice versa). [b] –829.7012 hartrees at the MP4SD2 level.

C_2H_4 Insertion into the Pt–SiH_3 Bond of 1A. C_2H_4 can be inserted into the Pt–SiH_3 bond in **1A** and **1C** and into the Pt–H bond in **1B** and **1C**. We will investigate first the C_2H_4 insertion into the Pt–SiH_3 bond of **1A**.

(12) Hay, P. J.; Wadt, W. R. *J. Chem. Phys.* **1985**, *82*, 299.
(13) Huzinaga, S.; Andzelm, J.; Klobukowski, M.; Radio-Andzelm, E.; Sakai, Y.; Tatewaki, H. *Gaussian basis sets for molecular calculations*; Elsevier: Amsterdam, 1984.
(14) Dunning, T. H.; Hay, P. J. In *Methods of Electronic Structure Theory*; Schaefer, H. F., Ed.; Plenum: New York, 1977; p 1.
(15) Van Duijneveldt, F. B. Gaussian Basis Sets for the Atoms H–Ne for Use in Molecular Calculations. *IBM J. Res. Dev.* **1971**, 945.
(16) Sakai, Y.; Tatewaki, H.; Huzinaga, S. *J. Comput. Chem.* **1981**, *2*, 108.
(17) Optimized bond angles are given in the supplementary material.

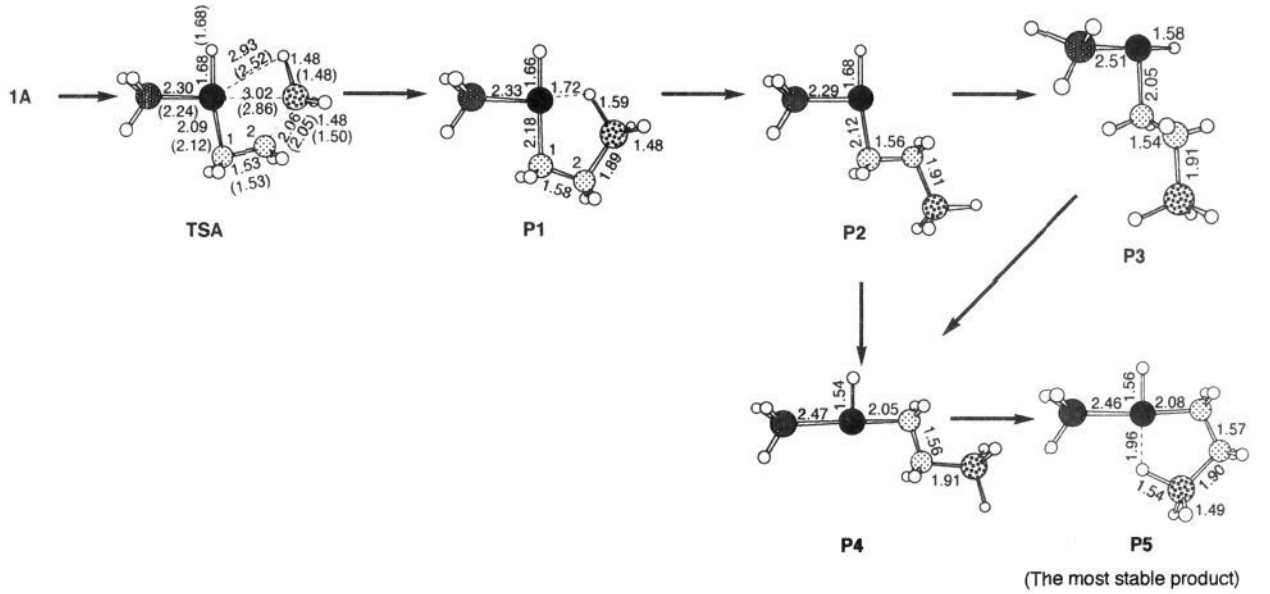

Figure 2. Optimized geometries of the transition state **TSA** and products of the C_2H_4 insertion into the Pt–SiH_3 bond of $PtH(SiH_3)(PH_3)(C_2H_4)$ (**1A**). (See Figure 1 for **1A**. The MP2-optimized values are given in parentheses.) Bond lengths in Å. Bond angles are omitted here.[17]

Optimized geometries of transition state (**TSA**) and possible products (**P1**–**P5**) are shown in Figure 2.[17] At **TSA**, C_2H_4 moves toward SiH_3, the Pt–C^1 distance (2.09 Å) is considerably short, like it is in **P1**, and the C^1–C^2 distance (1.53 Å) is only 0.05 Å shorter than it is in **P1**. The Pt–SiH_3 distance is considerably long, the SiH_3 group is changing its direction toward C_2H_4, and the Si–C^2 distance (2.06 Å) is only 0.17 Å longer than that in **P1**. All these features indicate that **TSA** is product-like and that the Pt–(σ-alkyl) bond is already formed at **TSA**. The Pt–PH_3 distance becomes shorter but the Pt–H distance becomes longer at **TSA**. These geometrical changes are interpreted in terms of trans-influence: because the Pt–SiH_3 bond is getting longer in the reaction, the trans-influence of SiH_3 is getting less effective, which strengthens the Pt–PH_3 bond. On the other hand, the Pt–H bond is getting weaker because the σ-alkyl group is gradually formed at the position trans to the Pt–H bond. Accordingly, the Pt–H bond becomes longer but the Pt–PH_3 bond becomes shorter in the reaction.

In **P1**, the distance between Pt and H^γ of SiH_3 is only 1.72 Å, suggesting that the Pt–H^γ agostic interaction is considerably strong. **P2**, in which the Pt–H^γ agostic interaction disappears (Figure 2), is calculated to be less stable than **P1** by ca. 19 kcal/mol (MP4SDQ). This value slightly increases to 19.7 kcal/mol when a p-function is added to the basis set of H^γ. Thus, the strength of the Pt–H^γ agostic interaction in **P1** is estimated to be ca. 19 kcal/mol.

Although **TSA** of this reaction is product-like, the Pt–H^γ agostic interaction is not yet formed at **TSA**. To examine carefully the agostic interaction in **TSA**, we reoptimized the geometry of **TSA** at the MP2 level (see values in parentheses of Figure 2). The Pt–H^γ distances becomes shorter (2.52 Å), but it is still too long to form the agostic interaction. Furthermore, the Si–H^γ bond distance (1.48 Å) is almost the same as the other Si–H bond distances. These geometrical features clearly show that **TSA** does not involve the Pt–H^γ agostic interaction. The activation energy (E_a) was calculated at the MP4SDQ level to be 53.9 kcal/mol for the HF-optimized geometry and 56.5 kcal/mol for the MP2-optimized geometry (Table 2).

The reductive elimination of H–$CH_2CH_2SiH_3$, which must occur to complete the hydrosilation of alkene, cannot take place in **P1** and **P2**. Besides **P1** and **P2**, there are three possible products (**P3**–**P5** in Figure 2) in which the reductive elimination can occur. In them, **P5** is the most stable, because the trans-position of the H ligand is empty and the strong Pt–H^γ agostic interaction is involved in **P5**. **P5** is, however, less stable than **1A** by 12.8 kcal/mol (MP4SDQ).

Table 2. Energy Changes by C_2H_4 Insertion into Pt–SiH_3 or Pt–H Bond (kcal/mol)[a]

complex[b]	HF	MP2	MP3	MP4DQ	MP4SDQ
	(A) C_2H_4 Insertion into Pt–SiH_3 of **1A**				
1A	0.0[c]	0.0[d]	0.0[e]	0.0[f]	0.0[g]
TSA	45.9	54.9	50.2	53.4	53.9
P1	21.7	31.3	27.0	29.8	30.5
P2	32.8	51.4	44.7	48.4	49.3
P3	12.5	23.0	18.0	20.6	21.5
P4	8.6	20.4	15.0	17.9	18.9
P5	6.4	13.8	9.7	12.1	12.8
	(B) C_2H_4 Insertion into Pt–H of **1B**				
1B	0.0[h]	0.0[i]	0.0[j]	0.0[k]	0.0[l]
TSB	20.1	19.7	18.6	20.3	20.6
P6	20.1	20.0	19.7	20.5	20.8
P7	26.6	40.5	33.9	36.8	37.6
P8	1.3	5.7	2.3	3.8	4.3
P9	–8.7	–6.1	–7.9	–6.7	–6.5
P10	–6.8	–4.8	–6.5	–5.3	–5.1
	(C) C_2H_4 Insertion into Pt–SiH_3 of **1C**				
1C	0.0[m]	0.0[n]	0.0[o]	0.0[p]	0.0[q]
TSC	17.8	16.2	15.0	16.2	16.3 (16.3)[r]
P5	–6.3	2.4	–2.0	–0.2	0.6 (2.9)
	(D) C_2H_4 Insertion into Pt–H of **1C**				
1C	0.0[m]	0.0[n]	0.0[o]	0.0[p]	0.0[q]
TSD	5.1	4.0	4.6	4.6	4.4 (4.2)
P10	–21.6	–19.7	–19.4	–18.6	–18.4
P9	–23.5	–18.0	–20.8	–20.0	–20.0 (–17.2)

[a] A positive value means destabilization in energy (and vice versa). [b] See Figures 2, 4, and 6. [c] –829.1277. [d] –829.6405. [e] –829.6657. [f] –829.6902. [g] –829.7011. [h] –829.1304. [i] –829.6395. [j] –829.6659. [k] –829.6903. [l] –829.7012. [m] –829.1074. [n] –829.6224. [o] –829.6470. [p] –829.6707. [q] –829.6817. [r] In parentheses are values from MP4SDTQ (–829.7040 for **1C**). All these values are given in hartrees.

Isomerization from **P1** to **P5** would occur after loss of the Pt–H^γ agostic interaction because the Pt–H^γ agostic interaction would suppress the isomerization. Thus, we examined the isomerization using $PtH(CH_3)(PH_3)$ as a model. Geometries of **P2′**, **P3′**, and **P4′** and transition states of the isomerizations are given in Figure 3,[17] where **P2′**, etc., means a model of **P2**, etc. As shown in Figure 3, **P2′** isomerizes to **P3′** with E_a of 11.6 kcal/mol at the HF level and E_a of 2.8 kcal/mol at the MP4SDQ level, and then **P3′** isomerizes to **P4′** with E_a of 6.8 kcal/mol at

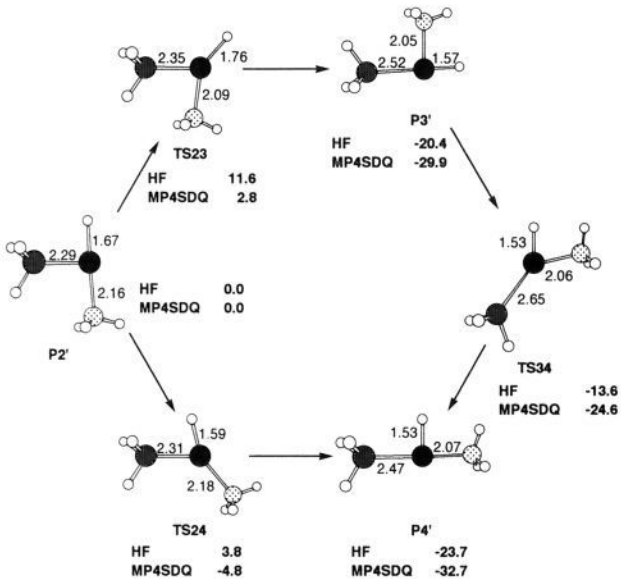

Figure 3. Optimized geometries of three isomers of $PtH(CH_3)(PH_3)$ and the transition states of isomerization between them. Bond lengths in Å. Bond angles are omitted here.[17]

the HF level and E_a of 5.3 kcal/mol at the MP4SDQ level. On the other hand, **P2'** directly isomerizes to **P4'** (the most stable isomer) with E_a of 3.8 kcal/mol at the HF level but no barrier at the MP4SDQ level. Thus, **P1** would isomerize to **P4** with no barrier immediately when the agostic interaction of 19 kcal/mol is lost. Further isomerization from **P4** to **P5** would occur very easily, because only a rotation around the C–C bond is necessary in the isomerization. Because deinsertion of ethene from **P1** to **1A** needs E_a of 23 kcal/mol (Table 2), isomerization from **P1** to **P5** occurs more easily than the deinsertion.

In conclusion, the C_2H_4 insertion into Pt–SiH_3 of **1A** occurs with a significantly high activation energy of 54 kcal/mol to yield **P1**, followed by further isomerization to **P5** to complete the hydrosilation of ethene, as summarized in Scheme 1(A). Thus, this reaction is very difficult.

C_2H_4 Insertion into the Pt–H Bond of 1B. Optimized geometries of transition state (**TSB**) and products (**P6–P10**) are shown in Figure 4.[17] At **TSB**, the C–C, Pt–C, and C–H distances are almost the same as those of **P6**, and an energy difference between **TSB** and **P6** is very small (Table 2). These results indicate that **P6** easily causes deinsertion of ethene with nearly no barrier. This is probably because the alkyl group is formed at the trans-position of SiH_3 (remember that trans-influence of alkyl and SiH_3 ligands is very strong). In both **TSB** and **P6**, the Pt–H^β distance (about 1.8 Å) is only 0.1–0.2 Å longer than the Pt–H bond of **1B**, and the C–H^β distance (1.25 Å) is much longer than the usual C–H bond distance. These geometrical features indicate that a strong Pt–H^β agostic interaction is involved in **TSB** and **P6**. The strength of this agostic interaction is estimated to be ca. 17 kcal/mol because **P6** is 16.8 kcal/mol more stable than **P7**, which does not involve this agostic interaction. In spite of

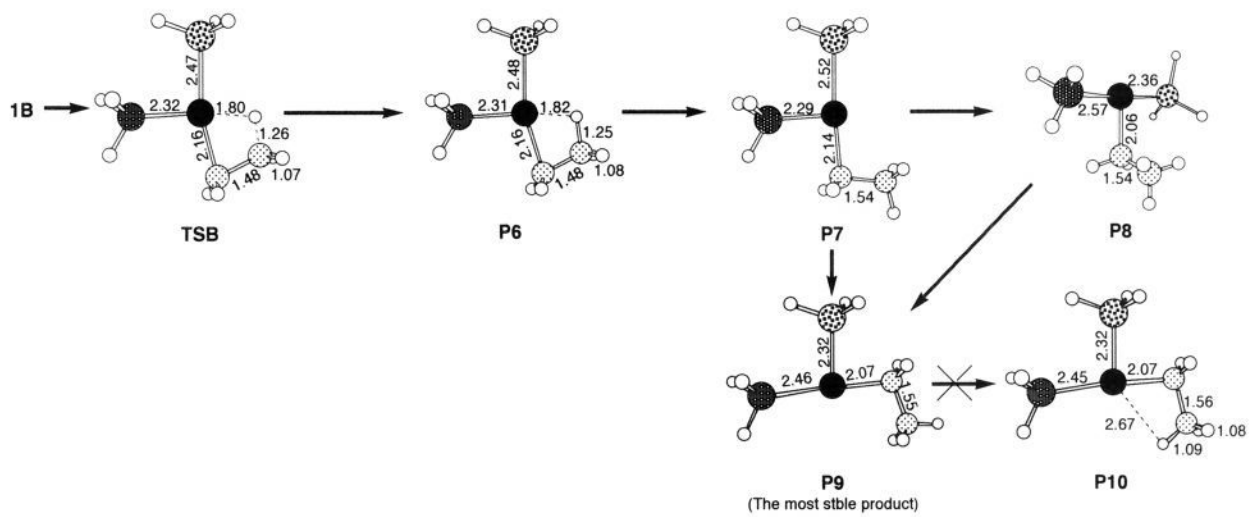

Figure 4. Optimized geometries of the transition state **TSB** and products of the C_2H_4 insertion into the Pt–H bond of $PtH(SiH_3)(PH_3)(C_2H_4)$ (**1B**). (See Figure 1 for **1B**.) Bond lengths in Å. Bond angles are omitted here.[17]

Scheme 1[a]

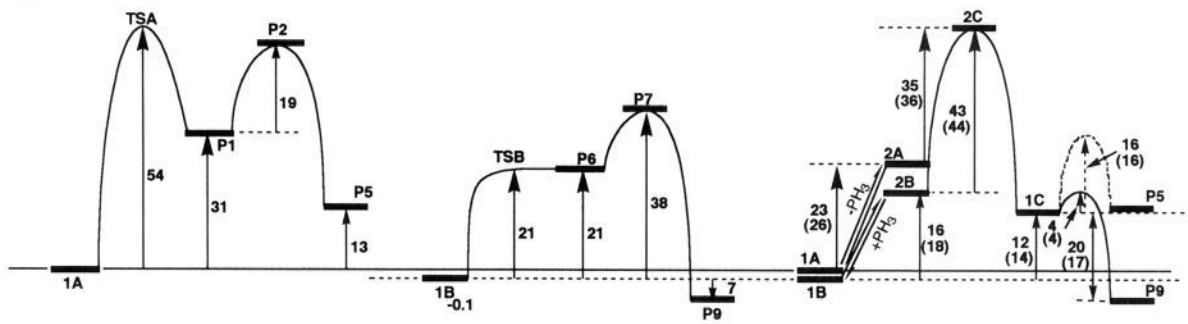

(A) C_2H_4 insertion into Pt-SiH_3 in **1A** (B) C_2H_4 insertion into Pt-H in **1B** (C) C_2H_4 insertion into Pt-H (solid line) or Pt-SiH_3 (dotted line) in **1C**

[a] Numbers represent energy difference in kcal/mol from MP4SDQ. Those in parentheses are from MP4SDTQ.

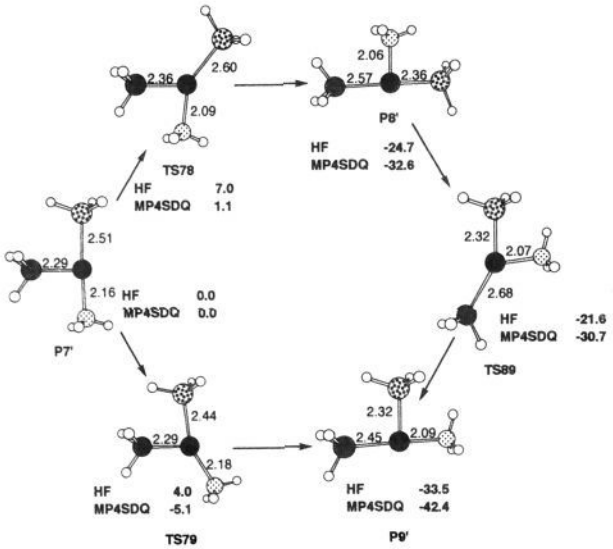

Figure 5. Optimized geometries of three isomers of $Pt(CH_3)(SiH_3)(PH_3)$ and the transition states of isomerization between them. Bond lengths in Å. Bond angles are omitted here.[17]

this strong agostic interaction, both **TSB** and **P6** are significantly less stable than **1B** by ca. 21 kcal/mol.

The reductive elimination of $H_3Si–CH_2CH_3$, which must occur to complete the hydrosilation of alkene, cannot take place in **P6** and **P7**. Besides **P6** and **P7**, there are three isomers, **P8**, **P9**, and **P10** (Figure 4), in which the reductive elimination can occur. In them, **P9** is the most stable, since the trans-position to SiH_3 is empty. The Pt–H^β agostic interaction is not involved in it, probably because SiH_3 lying at the trans-position of H^β disfavors the formation of agostic interaction due to its strong trans-influence. **P9** is 6.5 kcal/mol more stable than **1B** (Table 2). Thus, insertion **1B** → **P9** is exothermic.

We next investigate isomerization from **P6** to **P9**. This isomerization would occur after loss of the agostic interaction in **P6**, because the agostic interaction suppresses the isomerization. Thus, we examined isomerization from **P7** to **P9**, using $Pt(PH_3)(SiH_3)(CH_3)$ as a model. Optimized geometries of $Pt(PH_3)(SiH_3)(CH_3)$ and the TS of the isomerization are shown in Figure 5.[17] The activation energy was calculated to be 7.0 kcal/mol at the HF level and 1.1 kcal/mol at the MP4SDQ level for isomerization from **P7'** to **P8'**, 3.1 kcal/mol at the HF level and 1.9 kcal/mol at the MP4SDQ level for isomerization from **P8'** to **P9'**, and 4.0 kcal/mol at the HF level and no barrier at the MP4SDQ level for the direct isomerization from **P7'** to **P9'** (the most stable product). Thus, isomerization from **P6** to **P9** would easily occur with nearly no barrier after loss of the Pt–H^β agostic interaction. About 17 kcal/mol (MP4SDQ) is necessary to break the agostic interaction (remember that the strength of the Pt–H^β agostic interaction is about 17 kcal/mol). This value is higher than the activation barrier of the de-insertion of ethene (vide supra).

In conclusion, ethene is inserted into the Pt–H bond with an activation energy of 21 kcal/mol, to yield **P6**, followed by isomerization **P6** → **P9** which causes energy destabilization of 17 kcal/mol to break the Pt–H^β agostic interaction. The total activation energy for reaction **1B** → **P9** is 38 kcal/mol (= 21 + 17 kcal/mol),[18] as shown in Scheme 1(B). These results lead to the conclusion that C_2H_4 is much more easily inserted into the Pt–H bond of **1B** than it is into the Pt–SiH_3 bond of **1A**.

C_2H_4 Insertion into the Pt–H or Pt–SiH_3 Bond of 1C. In **1C**, ethene is inserted into the Pt–SiH_3 bond, to yield product **P5** through transition state **TSC** (Figure 6).[17] **TSC** resembles **TSA**, while **TSC** includes a shorter C–C distance and a longer C–Si distance than those of **TSA**. Because **P5** is the most stable in $PtH(PH_3)(CH_2CH_2SiH_3)$ and can cause reductive elimination of $H–CH_2CH_2SiH_3$ (see above), we do not need to consider any isomerization. As shown in Table 2, this insertion occurs with an activation energy of 16.3 (16.3) kcal/mol and endothermicity of 0.6 (2.9) kcal/mol at the MP4SDQ level, where results at the MP4SDTQ level are given in parentheses.

The C_2H_4 insertion into the Pt–H bond occurs through transition state **TSD**, yielding product **P10** (Figure 6). The geometry of **TSD** differs somewhat from that of **TSB**; for instance, the C–C distance is considerably shorter, and the C–H distance is much longer, but the Pt–H distance is shorter than those in **TSB**, indicating that **TSD** is relatively reactant-like. **P10** is slightly less stable than **P9** (vide supra). However, isomerization **P10** → **P9** needs only the rotation around the C–C bond, which would occur with no barrier. Thus, **TSD** is the true transition state of reaction **1C** → **P9**, and this reaction takes place with E_a of 4.4 (4.2) kcal/mol and E_{exo} of 20.0 (17.2) kcal/mol at the MP4SDQ level (Table 2), where the MP4SDTQ results are given in parentheses.

In conclusion, ethene is easily inserted into the Pt–H and Pt–SiH_3 bonds in **1C**, and the insertion into the Pt–H bond occurs more easily than that into the Pt–SiH_3 bond, as shown in Scheme 1(C).

Factors Determining the Energy of Reaction (ΔE). In the C_2H_4 insertion into the Pt–SiH_3 bond, the Si–C and Pt–C bonds are newly formed, but the Pt–SiH_3 bond is broken. In the C_2H_4 insertion into the Pt–H bond, the C–H and Pt–C bonds are newly formed, but the Pt–H bond is broken. Thus, the difference in ΔE between two insertion reactions would depend on these bond energies (note that the change of a C=C double bond to a C—C single bond is common in all the insertion reactions examined). These bond energies have been estimated in our previous theoretical work[19] on the basis of following reactions.

$$Pt(PH_3)_2 + H_2 \rightarrow \textit{cis}\text{-}Pt(H)_2(PH_3)_2 \quad (2)$$

$$Pt(PH_3)_2 + CH_3CH_3 \rightarrow \textit{cis}\text{-}Pt(CH_3)_2(PH_3)_2 \quad (3)$$

$$Pt(PH_3)_2 + SiH_3–SiH_3 \rightarrow \textit{cis}\text{-}Pt(SiH_3)_2(PH_3)_2 \quad (4)$$

$$H–CH_3 \rightarrow {}^\bullet H + {}^\bullet CH_3 \quad (5)$$

$$H_3Si–CH_3 \rightarrow {}^\bullet SiH_3 + {}^\bullet CH_3 \quad (6)$$

As is clearly shown in Scheme 2, the E(Pt–Si) value is similar to the E(Pt–H) value, but the E(C–H) value is larger than the E(Si–C) value. From these results, one might conclude that the C_2H_4 insertion into the Pt–H bond is more exothermic (or less endothermic) than that into the Pt–SiH_3 bond because the former yields the stronger C–H bond and the latter the weaker Si–C bond. To certify this conclusion, we compare several reactions whose products do not involve agostic interaction. Certainly, reaction of **1B** → **P9** (C_2H_4 insertion into the Pt–H bond; E_{exo} = ca. 7 kcal/mol) is more exothermic than reaction of **1A** → **P4** (C_2H_4 insertion into the Pt–SiH_3 bond; E_{endo} = ca. 19 kcal/mol) (Table 2); the difference in ΔE between these two reactions roughly corresponds to the difference between C–Si and C–H bond energies. Also, reaction of **1C** → **P9** (C_2H_4 insertion into the Pt–H bond; E_{exo} = ca. 20 kcal/mol) is more exothermic than reaction of **1C** → **P4** (C_2H_4 insertion into the Pt–SiH_3 bond;

(18) The other aspect seems possible, as follows. Because **P6** is less stable than **1B** by 21 kcal/mol and there is no activation barrier between them, **P6** considered to be in thermal equilibrium with **1B**. If so, the activation energy to yield **P9** is about 17 kcal/mol.

(19) (a) Sakaki, S.; Ieki, M. *J. Am. Chem. Soc.* **1993**, *115*, 2373. (b) E(Pt–SiH_3) reported in ref 19a was slightly larger than the present value because of our careless miss in ref 19a. (c) These values differ from those in ref 19a because a p-polarization function is added to H in the present work.

(20) Walsh, R. *Acc. Chem. Res.* **1981**, *14*, 246.

(21) Golden, D. M.; Benson, S. W. *Chem. Rev.* **1969**, *69*, 125.

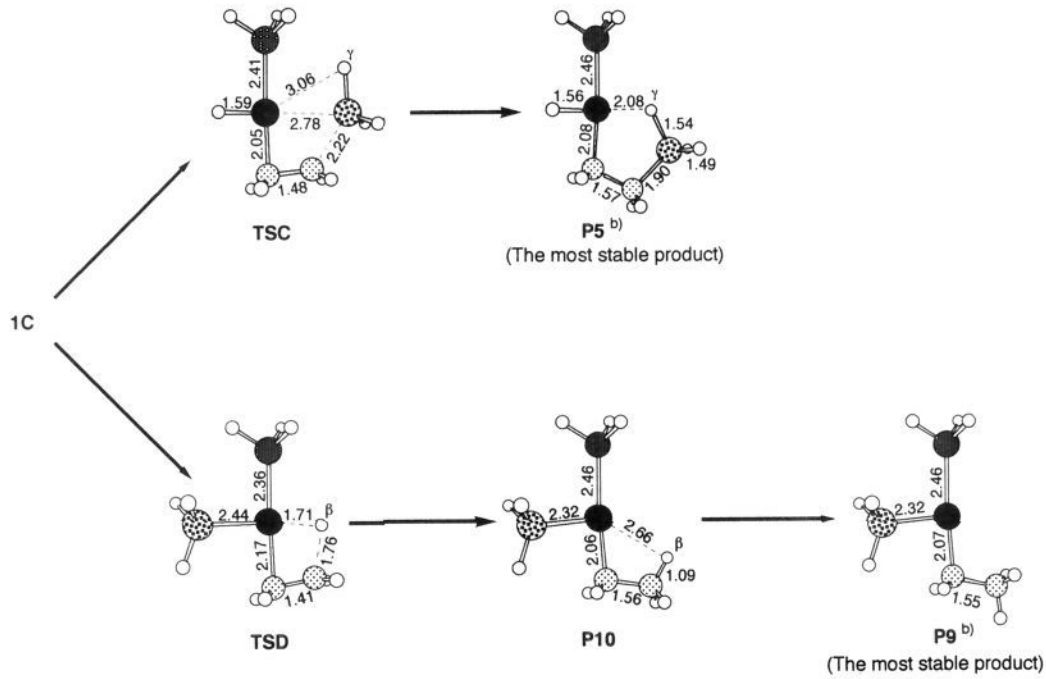

Figure 6. Optimized geometries of the transition states **TSC** and **TSD** and products of the C_2H_4 insertion into either the Pt–SiH_3 or Pt–H bond of **1C**. (See Figure 1 for **1C**). Bond lengths in Å. Bond angles are omitted here.[17] Orientation of PH_3 is different from that of **P5** and **P10** shown in Figures 2 and 4.

Scheme 2[a]

$Pt(H)(SiH_3)(PH_3)(C_2H_4) \longrightarrow Pt(H)(CH_2CH_2SiH_3)(PH_3)$

	E(Pt-SiH_3)	E(Pt-CH_3)	E(C-Si)
MP2	58	42	83
MP3	55	40	81
MP4DQ	56	40	80
MP4SDQ	56	40	81
MP4SDTQ	58	41	82
			(88.2)[20]

$Pt(H)(SiH_3)(PH_3)(C_2H_4) \longrightarrow Pt(SiH_3)(CH_2CH_3)(PH_3)$

	E(Pt-H)	E(Pt-CH_3)	E(C-H)
MP2	60	42	107
MP3	62	40	108
MP4DQ	62	39	108
MP4SDQ	62	40	108
MP4SDTQ	61	41	108
			(104)[21]

$PtH(CH_3)(PH_3)(C_2H_4) \longrightarrow PtH(CH_2CH_2CH_3)(PH_3)$

	E(Pt-CH_3)	E(Pt-CH_3)	E(C-C)
MP2	42	42	87
MP3	42	42	85
MP4DQ	39	39	85
MP4SDQ	40	40	85
MP4SDTQ	41	41	86
			(88)[20]

[a] Values are given in kcal/mol. Experimental values are in parentheses. See ref 19.

E_{endo} = ca. 9 kcal/mol). Some discrepancies between the difference in ΔE and the difference in bond energies would be due to the trans-influence and strengthening of the Pt–SiH_3 bond by the reaction **1C** → **P9** (similar discussion is given below).

The next important factor is the trans-influence of the ligand. For instance, relative stabilities of **P2**, **P3**, and **P4** depend on the ligand lying at the position trans to the Pt–C bond; **P2** is the least stable because the H ligand lies at the position trans to the Pt–C bond (Figure 2). On the other hand, the trans-position of the Pt–C bond is empty in **P3** but occupied by PH_3 in **P4** (remember, the trans-influence becomes stronger in the order $PH_3 \ll H < SiH_3$). Similarly, relative stabilities of **P7**, **P8**, and **P9** are determined by the ligand lying at the trans-position of SiH_3; in these complexes, **P9** is the most stable because the trans-position of SiH_3 is empty (Figure 4), **P8** is the next most stable because the trans-position of C_2H_5 is empty but the trans-position of SiH_3 is occupied by PH_3, and **P7** is the least stable because two strong C_2H_5 and SiH_3 ligands lie trans to each other.

The third important factor is the agostic interaction. Its strength depends on the ligand lying at the trans-position of the agostic interaction. For instance, the strength of the Pt–H^γ agostic interaction is estimated to be ca. 19 kcal/mol when PH_3 lies at the position trans to the Pt–H^γ interaction (compare **P1** and **P2** in Figure 2), but only ca. 6 kcal/mol when H is at the position trans to this interaction (compare **P4** and **P5** in Figure 2). The strength of Pt–H^β agostic interaction is estimated to be 17 kcal/mol when PH_3 lies at the position trans to the Pt–H^β interaction (compare **P6** and **P7** in Figure 4) but almost zero when SiH_3 lies at the position trans to this interaction (compare **P9** and **P10** in Figure 4).

Considering the three factors mentioned above, we can explain the ΔE value of the insertion reaction. The most exothermic reaction is the C_2H_4 insertion into the Pt–H bond, **1C** → **P9**. This is because the strong C–H bond is formed and the trans-position of SiH_3 is empty in **P9** (Figure 4). The next is the C_2H_4 insertion into the Pt–SiH_3 bond, **1C** → **P5** (Figure 6). This reaction is less exothermic than reaction of **1C** → **P9**, because this insertion produces the weak Si–C bond. Although the Pt–H^γ agostic interaction is involved in **P5**, this agostic interaction yields energy stabilization of only 6 kcal/mol, which is much smaller than the difference between E(C–H) and E(Si–C) values; accordingly, the agostic interaction does not reverse the order of exothermicity of reactions **1C** → **P9** and **1C** → **P5**.

The C_2H_4 insertion into the Pt–H bond of **1B** → **P9** is exothermic (6.5 kcal/mol), but the C_2H_4 insertion into the Pt–SiH_3 bond of **1A** → **P5** is endothermic (12.8 kcal/mol); the former produces the weak Si–C bond but the latter the strong C–H bond. However, reaction **1A** → **P5** yields additional energy stabilization (ca. 6 kcal/mol) by the Pt–H^γ agostic interaction. Also, reaction **1B** → **P9** yields additional stabilization of the Pt–SiH_3 bond, as follows. The Pt–SiH_3 distance shortens to 2.32 Å (in **P9**) from 2.36 Å (in **1B**) in reaction **1B** → **P9** (Figure 4), whereas the Pt–H distance changes little in reaction **1A** → **P5** (Figure 2). These geometry changes indicate that the Pt–SiH_3 bond would strengthen in reaction **1B** → **P9** but the Pt–H bond would not in reaction **1A** → **P5** and that strengthening of the

$Pt–SiH_3$ bond would yield additional stabilization in **P9**. This additional stabilization would correspond to the additional stabilization of **P5** by the $Pt–H^{\gamma}$ agostic interaction. Thus, the difference in ΔE between these two reactions (ca. 19 kcal/mol) is roughly in accord with the difference between E(Si–C) and E(C–H) bond energies (ca. 20 kcal/mol).

Reaction of **1A** → **P5** is more endothermic than reaction of **1C** → **P5**. Both involve C_2H_4 insertion into the $Pt–SiH_3$ bond. The difference is, therefore, interpreted in terms of trans-influence of H and PH_3. SiH_3 lies at the trans-position of PH_3 in **1A** and at the trans-position of H in **1C**. Because this unfavorable situation of **1C** disappears in the product, reaction of **1C** → **P5** is less endothermic than reaction of **1A** → **P5**. The difference in ΔE between reactions **1B** → **P9** and **1C** → **P9** can be explained in a similar way.

Determining Factors for the Activation Energy (E_a). In **1C**, ethene is inserted into the Pt–H bond with a lower activation energy than that into the $Pt–SiH_3$ bond. This result is again interpreted in terms of bond energies. The stronger C–H bond is formed in the former, while the weaker Si–C bond is formed in the latter; accordingly, the former E_a is lower than the latter E_a. The next factor is the directionality of valence orbitals of H and SiH_3;[22] as has been pointed previously,[19] SiH_3 has a directional sp^3 valence orbital but H has a spherical 1s orbital. At the TS, the $Pt–SiH_3$ bond must be broken to form a new bond with C_2H_4, while the H ligand can start to interact with C_2H_4, keeping the Pt–H bond. This is one of the reasons that the C_2H_4 insertion into the $Pt–SiH_3$ bond requires a higher E_a than does that into the Pt–H bond. The third factor is trans-influence of the ligand lying at the trans-position of C_2H_4. E_a of reaction **1B** → **P6** (Figure 4) is much higher than E_a of reaction **1C** → **P9** (Figure 6). Because both reactions involve C_2H_4 insertion into the Pt–H bond, this difference cannot be explained in terms of bond energy and directionality of the valence orbital. In **TSB** of reaction **1B** → **P6**, the Pt–C σ-bond is already formed at the trans-position of SiH_3. In **TSD** of reaction **1C** → **P9**, on the other hand, the Pt–C σ-bond is getting formed at the trans-position of PH_3. Apparently, **TSD** is more favorable than **TSB** from the viewpoint of trans-influence. Also, the difference between two insertion reactions into the $Pt–SiH_3$ bond can be explained in a similar way, as follows: reaction **1A** → **P1** requires a higher activation energy than reaction **1C** → **P9**, because the former yields the Pt–C σ-bond at the trans-position of H but the latter yields it at the trans-position of PH_3. These results indicate that the C_2H_4 insertion occurs easily when the ligand lying at the trans-position to C_2H_4 exerts weak trans-influence. The agostic interaction also stabilizes **TSB** of reaction **1B** → **P6**, while TSs of the other insertion reactions hardly receive energy stabilization from this interaction.

In conclusion, the activation energy is mainly determined by bond energy, the directionality of valence orbitals of H and SiH_3, the ligand lying at the trans-position of C_2H_4, and sometimes the agostic interaction.

Based on the above discussion, we can compare the C_2H_4 insertion into the $Pt–CH_3$ bond with that into the $Pt–SiH_3$ and Pt–H bonds. In the C_2H_4 insertion into the $Pt–SiH_3$ bond, the strong $Pt–SiH_3$ bond changes to the weak $Pt–CH_2CH_2SiH_3$ bond,

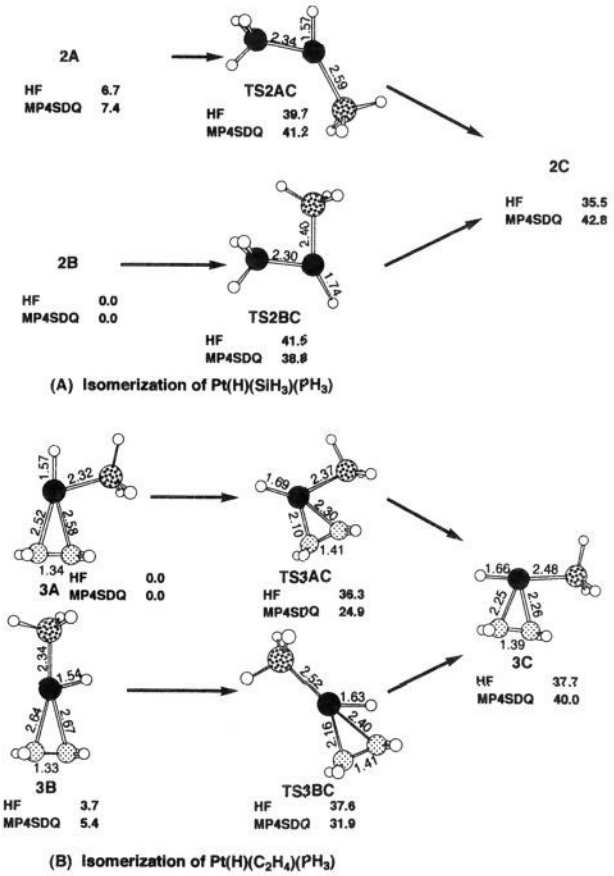

Figure 7. Isomerizations of $PtH(SiH_3)(PH_3)$ (**2**) and $PtH(SiH_3)(C_2H_4)$ (**3**). Bond lengths in Å. Bond angles are omitted here.[17]

as shown in Scheme 2. In the C_2H_4 insertion into the $Pt–CH_3$ bond, on the other hand, the $Pt–CH_3$ bond changes to a similar $Pt–CH_2CH_2CH_3$ bond. Thus, the C_2H_4 insertion into the $Pt–CH_3$ bond is more exothermic than that into the $Pt–SiH_3$ bond (note that E(C–C) is similar to E(C–Si)). In discussing the E_a value, we need to consider the directionality of valence orbitals of CH_3 and SiH_3. As is known,[22] both SiH_3 and CH_3 have a directional sp^3 valence orbital. This means that both $Pt–SiH_3$ and $Pt–CH_3$ bonds must be broken at the TS of the C_2H_4 insertion. Apparently, the weaker $Pt–CH_3$ bond is more easily broken than the stronger $Pt–SiH_3$ bond. From these results, we can predict that C_2H_4 is more easily inserted into the $Pt–CH_3$ bond with lower E_a than it is into the $Pt–SiH_3$ bond. In the C_2H_4 insertion into the Pt–H bond, the strong Pt–H bond must be broken but the strong C–H bond is formed, while the weak $Pt–CH_3$ bond is broken and the weak C–C bond is formed in the C_2H_4 insertion into the $Pt–CH_3$ bond. The difference between E(Pt–H) and E($Pt–CH_3$) is slightly larger than the difference between E(C–H) and E(C–C). Thus, we can suggest that the C_2H_4 insertion into the $Pt–CH_3$ bond is slightly more exothermic than that into the Pt–H bond. Although the $Pt–CH_3$ bond is weaker than the Pt–H bond, it is not easy to predict which proceeds with lower E_a, the C_2H_4 insertion into the $Pt–CH_3$ bond or the C_2H_4 insertion into the Pt–H bond, because CH_3 has a directional sp^3 valence orbital unlike the spherical 1s orbital of H.

Isomerization from 1A or 1B to 1C. We will address here isomerizations from **1A** and **1B** to **1C** because the C_2H_4 insertion in **1C** occurs most easily. This kind of isomerization can proceed through a three-coordinate intermediate. One possible intermediate is $PtH(SiH_3)(PH_3)$ (**2**) (Figure 1). C_2H_4 dissociates from **1A** to yield **2A**, with energy destabilization of 23 kcal/mol, and from **1B** to yield **2B**, with energy destabilization of 16 kcal/mol, as shown in Scheme 1(C) (hereafter, MP4SDQ values are given). Thus, **2A** and **2B** are considered to be in thermal

(22) Essentially the same discussion has been presented in previous reports of the H–H, $H–CH_3$, $CH_3–CH_3$, and $SiH_3–SiH_3$ oxidative additions to transition metals[22a–d] and the CO_2 insertion into the Cu–R bond (R = H or CH_3):[22e] (a) Blomberg, M. R. A.; Brandemark, U.; Siegbahn, P. E. M. *J. Am. Chem. Soc.* **1983**, *105*, 5557. (b) Saillard, J. Y.; Hoffmann, R. *J. Am. Chem. Soc.* **1984**, *106*, 2006. (c) Low, J. J.; Goddard, W. A. *Organometallics* **1986**, *5*, 609. Low, J. J.; Goddard, W. A. *J. Am. Chem. Soc.* **1986**, *108*, 6115. (d) Reference 23. (e) Sakaki, S.; Ohkubo, K. *Organometallics* **1989**, *8*, 2970.

(23) (a) The strong ligand tends to take an axial site in trigonal-bipyramidal structure.[23b,c] In $PtH(SiH_3)(PH_3)_2(C_2H_4)$, SiH_3 is the strongest ligand. Thus, the structure **4** (see text) is considered to be the most plausible species which is directly formed from **1A** and **1B**. (b) Rossi, A.; Hoffmann, R. *Inorg. Chem.* **1975**, *14*, 365. (c) Koga, K.; Jin, S. Q.; Morokuma, K. *J. Am. Chem. Soc.* **1988**, *110*, 3417.

equilibrium with **1A** and **1B**, respectively. TSs of isomerizations **2A** → **2C** and **2B** → **2C** could be optimized at the HF level but disappeared at the MP2–MP4SDQ levels (Figure 7A).[17] This means that **2C** converts into **2A** or **2B** with no barrier. PH_3 coordination to **2C**, however, yields **1C** as a stable species. Because **2C** is less stable than **2A** by 35 kcal/mol and **2B** by 43 kcal/mol, energies of 35 and 43 kcal/mol are necessary to yield **1C** from **2A** and **2B**, respectively. The other possible intermediate is $PtH(SiH_3)(C_2H_4)$ (**3**) (Figure 7B).[17] PH_3 dissociates from **1A** to yield **3A**, with energy destabilization of 24 kcal/mol, and from **1B** to yield **3B**, with energy destabilization of 30 kcal/mol. Although TSs of isomerizations of **3A** → **3C** and **3B** → **3C** could be optimized at the HF levels using BS I, these TSs disappeared at both HF and MP2-MP4SDQ levels using BS II. **3C** is less stable than **3A** by 40 kcal/mol and **3B** by 35 kcal/mol. Thus, isomerizations **1A** → **1C** through **3A** and **1B** → **1C** through **3B** require energy destabilizations of 40 and 35 kcal/mol, respectively. Reactions of **2A** → **2C** and **3B** → **3C** requires smaller energy destabilizations than reactions **3A** → **3C** and **3A** → **3C**, and formation of **2A** from **1A** needs smaller energy destabilization than that of **3B** from **1B**. In conclusion, the isomerization of **1A** to **1C** through **2A** occurs most easily, with E_a of ca. 35 kcal/mol, where **2A** is considered to be in thermal equilibrium with **1A** (Scheme 1(C)). This value is much lower than E_a of the C_2H_4 insertion into the Pt–SiH_3 bond of **1A**. Because the C_2H_4 insertion into the Pt–H bond of **1C** occurs with E_a of only 4 kcal/mol, the C_2H_4 insertion into the Pt–H bond takes place easily immediately when **1A** isomerizes to **1C** (Scheme 1(C)). This means that detection of **1C** is very difficult.

Isomerizations of **1A** and **1B** through a five-coordinate intermediate are also plausible, because a five-coordinate complex easily causes geometry change via Berry pseudorotation. $PtH(SiH_3)(PH_3)_2(C_2H_4)$ (**4**) is considered to be a possible candidate for such a five-coordinate species.[21] We tried to optimize **4**, but

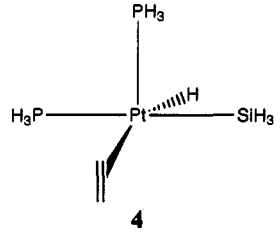

4

one PH_3 ligand on the equatorial site gradually dissociates from Pt during optimization. This suggests that formation of five-coordinate species would be difficult, although the possibility cannot be neglected completely. Even if the isomerization via five-coordinate species would occur with a lower activation energy than the isomerization via three-coordinate species, no change is made in the conclusion that the C_2H_4 insertion into the Pt–SiH_3 bond of **1A** requires a higher activation energy than the isomerization of **1A** → **1C**. When **1C** is formed, ethene is much more easily inserted into the Pt–H bond than it is into the Pt–SiH_3 bond (see above). In all cases, therefore, the C_2H_4 insertion into the Pt–SiH_3 bond is difficult. Because the isomerization through a five-coordinate intermediate must be investigated in more detail, we would like to investigate it in our future study.

IV. Concluding Remarks

The Pt-catalyzed hydrosilation of ethene occurs through the Chalk–Harrod mechanism, as follows. First, **1A** or **1B** is formed through oxidative addition of the Si–H σ-bond to Pt(0). Ethene is then inserted into the Pt–H bond of **1B** with an activation energy of ca. 21 kcal/mol (MP4SDQ), followed by isomerization to **P9**, from which the reductive elimination of H_3Si–CH_2CH_3 takes place to complete the hydrosilation of ethene. The total E_a is about 38 kcal/mol.[18] The other pathway, involving isomerization of **1A** to **1C**, seems possible. This isomerization would occur with an activation energy of ca. 35 kcal/mol. After the isomerization, ethene can be easily inserted into the Pt–H bond, with an activation energy of only 4 kcal/mol.

The C_2H_4 insertion into the Pt–SiH_3 bond is very difficult in **1A**, where its activation energy is 54 kcal/mol. In **1C**, also, this insertion is significantly more difficult than the C_2H_4 insertion into the Pt–H bond. Thus, the modified Chalk–Harrod mechanism does not work in the Pt-catalyzed hydrosilation of alkene.

Important factors determining the ease of the insertion are (1) the Si–C and C–H bond energies, (2) the trans-influence of the ligand lying at the trans-position of C_2H_4, (3) the directionality of the valence orbitals of SiH_3 and H, and sometimes (4) the agostic interaction between Pt and the C–H or Si–H bond. In $PtH(SiH_3)(PH_3)(C_2H_4)$, the Pt–H bond energy is almost the same as the Pt–SiH_3 bond energy. Thus, ethene is more easily inserted into the Pt–H bond than it is into the Pt–SiH_3 bond, because the C–H bond is stronger than the Si–C bond and the H ligand has a spherical 1s valence orbital. If the M–H bond is considerably stronger than the M–SiH_3 bond and the difference between M–H and M–SiH_3 bond energies sufficiently exceeds the difference between Si–C and C–H bond energies, then ethene would be inserted into the M–SiH_3 bond. In such a case, transition-metal-catalyzed hydrosilation of alkene would proceed through modified the Chalk–Harrod mechanism.

Acknowledgment. This work was supported in part by a grant from Ministry of Education, Culture, and Science (Grant-in-Aid Nos. 04243102 and 06227256). Calculations were carried out by using the Hitachi S-820 computer of the Institute for Molecular Science and the IBM RS-6000/340 workstation of our laboratory.

Supplementary Material Available: Optimized bond angles (2 pages). This material is contained in many libraries on microfiche, immediately follows this article in the microfilm version of the journal, and can be ordered from the ACS; see any current masthead page for ordering information.